4ICEGE Thessaloniki-GREECE 2007

4th International Conference on
Earthquake Geotechnical Engineering
June 25-28, 2007
Paper No. 1125

LIQUEFACTION-INDUCED SETTLEMENT OF RIVER LEVEE DUE TO LONG/SHORT GROUND EXCITATION

Masata SUGITO[1], Atsushi YASHIMA[2], Yu HUANG[3], Osamu NAKAYAMA[4], Satoshi TOKIWA[4], Tomoyuki ABE[5] , Genji SEKIZAWA[6] and Masumitsu KUSE[7]

ABSTRACT

The liquefaction potential of the main plain in the Chubu region is very high because the alluvial lowland is covered by loosely deposited sandy layers. A large settlement of the river levee on the alluvial lowland is expected and worried due to liquefaction during a large earthquake. The Tonankai-Tokai coupled earthquake is one of the most emergent candidate earthquakes attacking the Chubu region. Many active faults which generate severe excitations exist around the river levees on the alluvial lowland. In this study, effective stress based finite element analyses are carried out to compare the liquefaction-induced settlement of the river levees by both Tonankai-Tokai coupled and one representative active fault earthquakes. From the numerical results, it is found that the long-duration earthquake represented by Tonankai-Tokai coupled earthquake gives much large settlement of the river levee than the short-duration earthquake represented by the near-field active fault earthquake.

Keywords: liquefaction, numerical analysis, river levee, duration of strong motion, settlement

INTRODUCTION

In the Chubu region which is located in the center of Japan's main island, land areas below sea level are widely distributed in the lower reaches of the Kiso, Nagara, and Ibi Rivers (the Kiso Sansen downstream area). The liquefaction potential of the main plain in the Chubu region is very high because the alluvial lowland is covered by loosely deposited sandy layers. A large settlement of the river levee on the alluvial lowland is expected and worried due to liquefaction during a large earthquake. The Tonankai-Tokai coupled earthquake is one of the most emergent candidate earthquakes attacking the Chubu region. Many active faults, which generate severe excitations, exist around the river levees on the alluvial lowland. In this study, effective stress based finite element analyses are carried out by program code "LIQCA" (2005) to compare the liquefaction-induced settlement of the river levees by both Tokai-Tonankai and one representative active fault earthquakes.

Two input acceleration motions are prepared for the comparative simulations.

(1) Tonankai-Tokai coupled earthquake: The maximum acceleration is less than 250 gal at the engineering base and the duration is more than 100 seconds.
(2) Active fault earthquake: The maximum acceleration is about 600 gal at the engineering base and the duration is less than 10 seconds.

[1] Professor, River Basin Research Center, Gifu University, Japan, Email: sugito@gifu-u.ac.jp
[2] Professor, Department of Civil Engineering, Gifu University, Japan, Email: yashima@gifu-u.ac.jp
[3] Associate Professor, Department of Geotechnical Engineering, Tongji University, China
[4] Japan Institute of Construction, Japan
[5] OYO Corporation, Japan
[6] Ministry of LIT, Chubu Regional Bureau, Japan
[7] Assistant Professor, River Basin Research Center, Gifu University, Japan, Email: kuse@gifu-u.ac.jp

In the conventional design chart for the countermeasures against liquefaction, the liquefaction resistance factor, F_L, is used. If the soil condition is identical, the resistance factor is lower as the input acceleration is larger. Therefore the active fault earthquake is expected to induce much larger settlement of the crown of the river levee than Tonankai-Tokai coupled earthquake based on the conventional design method. In this study, the influence of the duration of earthquake excitation on the settlement mechanism of the river levee is discussed based on the comparative numerical analyses.

NUMERICAL SCHEME

Earthquake motion

Two acceleration motions were generated for the comparative simulation study on the effective stress based finite element analysis for the river levees. The two typical scenario earthquakes were selected. The fault models and the characteristics of the generated acceleration motions at the engineering base are in the following.

Fault Model of Scenario Earthquakes

The National Disaster Prevention Council (2001) and the Headquarter for Earthquake Research Promotion (HER, 2001) reported the models for the Tokai and Tonankai earthquakes, which have been identified as the most possible inter-plate earthquakes at the Nankai subduction zone. The occurrence possibility of their coupled earthquake in 30 years has been estimated as in the range of 60 ～90 %. The location of this coupled earthquake (Tonankai-Tokai coupled earthquake) as well as its epicenter and the asperity distribution on the fault plane represented by bold mesh are shown in Figure 1.

The other scenario earthquake selected for the comparative simulations is the inland active fault earthquake called Sekigahara-Yoro Fault earthquake. In Figure 1, the location of the fault and the simulation point at Kiso river mouth are shown. The fault parameters of these typical two scenario earthquakes are given in Table 1.

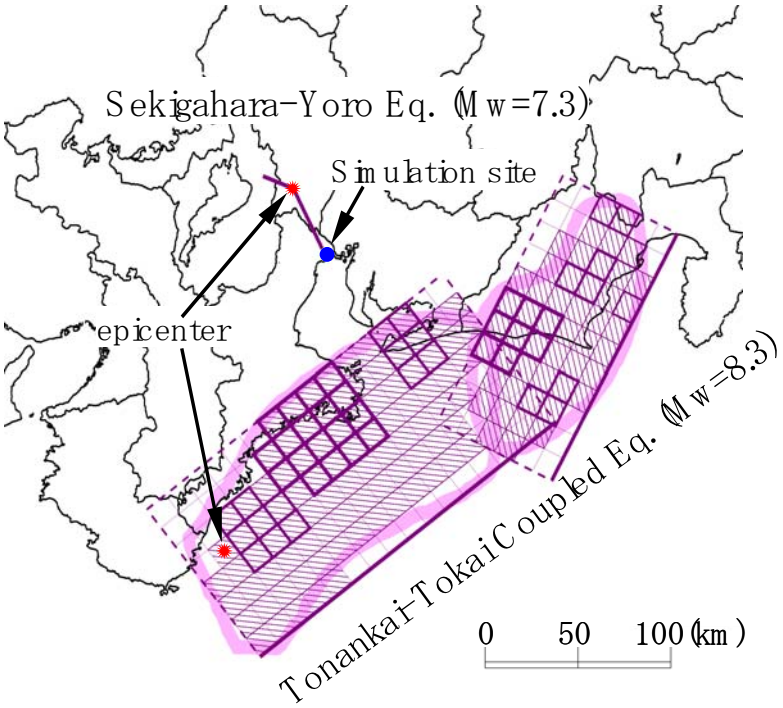

Figure 1. Location of scenario earthquakes and simulation site.

Acceleration Motions for Scenario Earthquakes

According to the fault parameters listed in Table 1, the acceleration time histories on the engineering base at the simulation site shown in Figure 2 were generated by using the simulation technique, EMPR (2000). In this technique, the acceleration time history from the given fault is simulated on the basis of the synthesis of the evolutionary power spectra that correspond to each individual sub-event equally divided on the fault. The effect of the asperity distribution on the fault into the ground acceleration time history is incorporated in the technique.

In Figure 2, the acceleration time histories for both scenario earthquakes are shown. As shown in Figure 2(a), the case for the Tonankai-Tokai coupled earthquake, the peak acceleration is not very high (Amax=235 cm/sec^2), however, the duration of motion is considerably long such as more than 100 seconds. This is the typical characteristic of strong motion for huge subduction earthquakes. On the other hand, in Figure 2(b), the peak acceleration is relatively high (Amax=594 cm/sec^2), and the duration of motion is very short such as less than 20 seconds. This is also the typical characteristic of near field strong motion for the inland active fault earthquakes.

Table 1. Fault parameters of scenario earthquakes.

		Tonankai-Tokai Coupled Eq.		Sekigahara-Yoro Eq.	
		Tonankai Fault	Tokai Fault	Sekigahara Fault	Yoro Fault
Hypocenter	Latitude	34° 12'10"		35° 20'59"	
	Longitude	137° 56'20"		136° 31'06"	
Fault Plane	Length L (km)	200	145	18	36
	Width W (km)	100	70	15	
	Area S (km^2)	21912		780	
	Strike θ (degree)	232.0	207.0	113.0	154.0
	Dip Angle δ (degree)	11.54	16.4	90.0	
Seismic Moment M_0 (Nm)		3.25×10^{21}		1.02×10^{20}	
Moment Magnitude M_w		8.3		7.0	
Propagation Velocity of Fault Rupture v_r (km/sec)		2.71		2.50	
Shear Wave Velocity V_{prop} (km/sec)		3.80		3.00	

Outline of LIQCA

The governing equations for the soil-water coupled problem are described based on Biot's two-phase mixture theory (Biot, 1941) and a *u-p* formulation is adopted in the 2-dimensional analysis, where *u* stands for the displacement and *p* is the pore water pressure. Equations (1) and (2) correspond the equation of motion and continuity equation for the Biot's two-phase mixture theory, respectively.

$$\rho\ddot{u}_i^s = \sigma_{ij,j} + \rho b_i \tag{1}$$

$$\rho^f \ddot{u}_{i,j}^s - p_{,ii} - \frac{\gamma_w}{k}\dot{\varepsilon}_{ii}^s + \frac{n\gamma_w}{kK^f}\dot{p} = 0 \tag{2}$$

Where ρ is the density of soils, $\ddot{u}_i^s$ is the acceleration of the solid, σ_{ij} is the total stress, b_i is the body force, ρ^f is the density of fluid, p is the pore water pressure, k is the permeability, K^f is the bulk modulus of the fluid and $\dot{\varepsilon}_{ii}^s$ is the volumetric strain of solid. The finite element method (FEM) is employed for the spatial discretization of the equation of motion while the finite difference method (FDM) is employed for the spatial discretization of the pore water pressure in continuity equation. The validity of the proposed numerical method was verified by Oka et al. (1994) through a comparison of the numerical results and the analytical solutions for a transient response of saturated porous solids. As to the constitutive model for sand, a cyclic kinematic elastoplastic model (Oka et al., 1999) is used and the detailed description of the model can be referred to the reference.

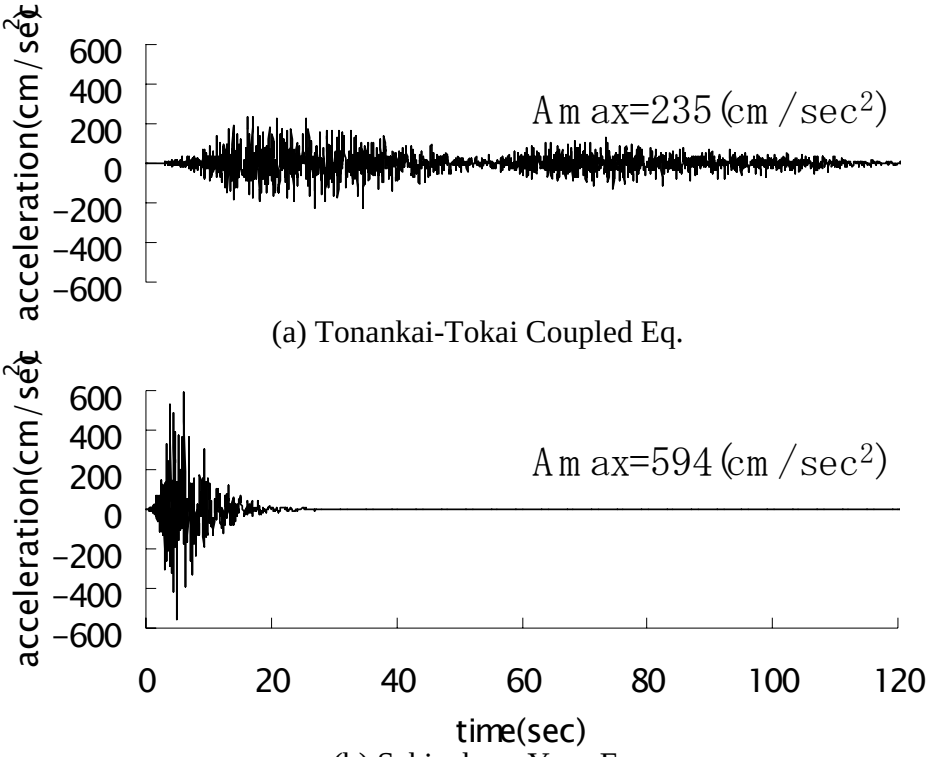

(a) Tonankai-Tokai Coupled Eq.

(b) Sekigahara-Yoro Eq.

Figure 2. Simulated acceleration time histories at engineering base.

River levee models

The reference problem shown in Figure 3 involves a 7 m high earth levee constructed on liquefiable soil at Kiso river left bank 4k000-point in the Chubu region, Japan. The numerical simulation uses the theoretical hypotheses of a plane strain condition. The finite element mesh consists of 2616 nodes, 2507 quadrilateral elements.

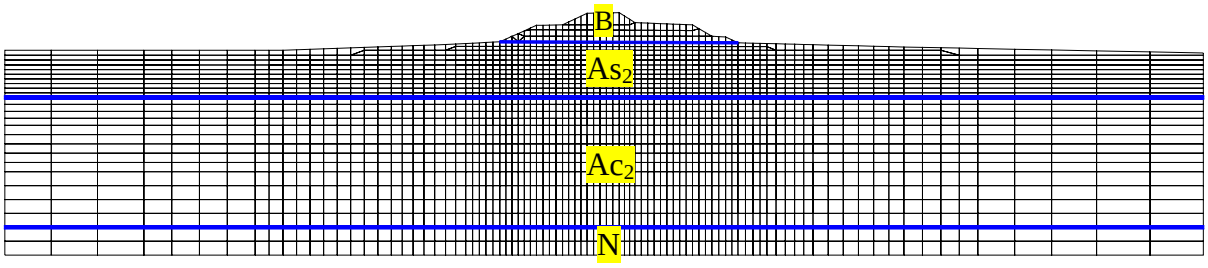

Figure 3. Finite element mesh of the river levee.

Soil parameters

The soil profile below the levee is also indicated in Figure 3. In this case, the soil layer 'As', typical alluvial sand, is liable to liquefaction as proved in the 1995 Hyogoken-Nambu Earthquake. The constitutive relation of the liquefiable sand is simulated using the aforementioned cyclic elastoplastic model. The corresponding parameters are defined taking into account typical experimental values based on the related geotechnical investigation. Figure 4 shows the simulated undrained response of saturated foundation soil under symmetric stress-controlled cyclic triaxial loading conditions, in terms of shear stress-strain and effective stress path. The coefficients of permeability of the fill material and alluvial sand layer are 9.1×10-5cm/s and that of alluvial clayey layer is 3.1×10-8cm/s. Those estimated values are obtained by the Creager's method (1945) based on particle size distributions. The liquefaction resistance of liquefiable soil B and As2 in Figure 3, is given according to the blow-count for the in situ soils. Figure 5 shows cyclic shear stress ratio for the soil B and As2.

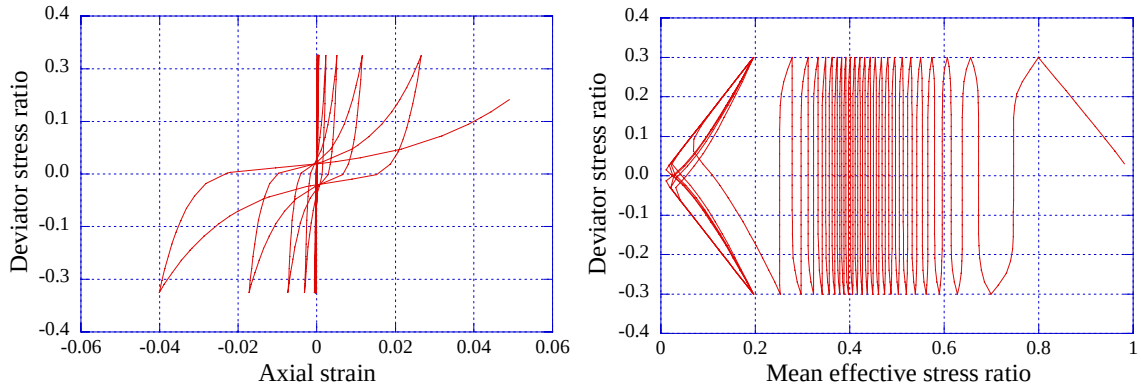

Figure 4. Numerical simulation of undrained response of the liquefiable sand.

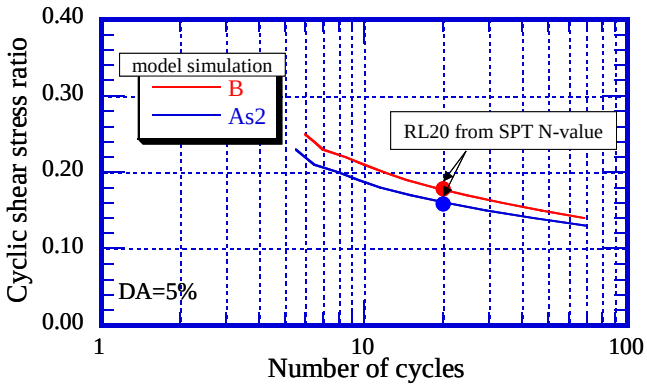

Figure 5. Liquefaction resistance of the in situ liquefiable soil.

Analytical conditions

The numerical simulation is carried out with the following boundary conditions:
(1) For the solid phase, a horizontal input motion is specified along the base. All base nodes are fixed in both vertical and horizontal directions. A simplified pseudo-free field boundary condition has been applied at the lateral boundaries, which implies that the displacements of the lateral side nodes equal those of the corresponding nodes at the same depths in free field. The similar boundary conditions have ever been used to simulate the tied node facility of laminar boxes (Zienkiewicz et al., 1999).
(2) For the pore pressures, the base and the two lateral sides are impervious. The ground surface is assumed as a drainage boundary.

The seismic loading is applied at the base of the levee-foundation system. In addition to hysteresis damping described by the cyclic elastoplastic constitutive model, Rayleigh damping proportional to the system-stiffness matrix is used with a damping ratio of 5%. For time stepping scheme, the Newmark method is used with $\beta = 0.3025$ and $\gamma = 0.6$. Time step is taken as 0.001 s.

A static elastic-perfectly plastic analysis with the Drucker-Prager yield criterion was performed to determine the distribution of initial stress field under gravity before seismic excitations.

NUMERICAL RESULTS AND DISCUSSIONS

In this section, computed excess pore water pressures, accelerations, deformations, and soil stress-strain response under both Tonankai-Tokai coupled earthquake and Sekigahara-Yoro earthquake are presented and compared with focus on some representative spatial locations.

Excess Pore water pressures

The distribution of excess pore water pressure ratios (the ratio of excess pore water pressure to initial effective vertical stress) at the end of the earthquake in the foundation soil is depicted in Figure 6.

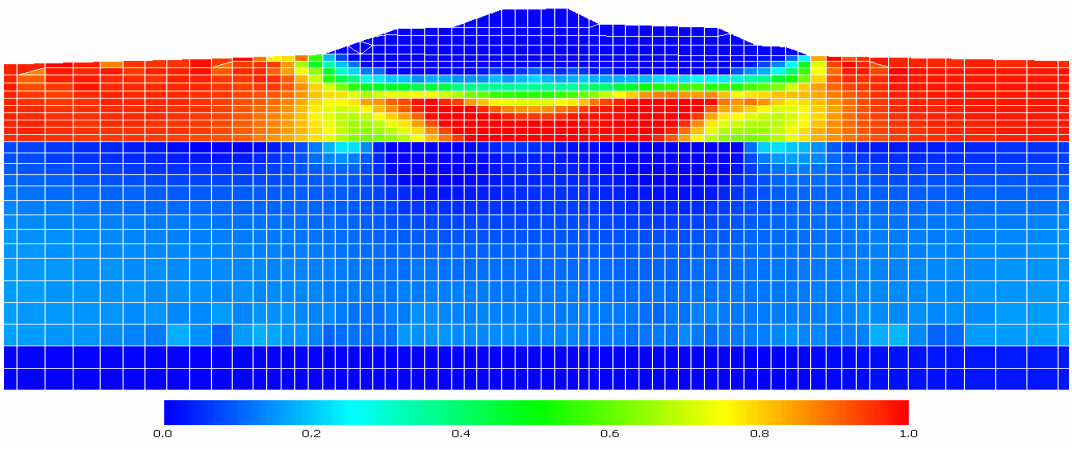

(a) Sekigahara-Yoro Eq.

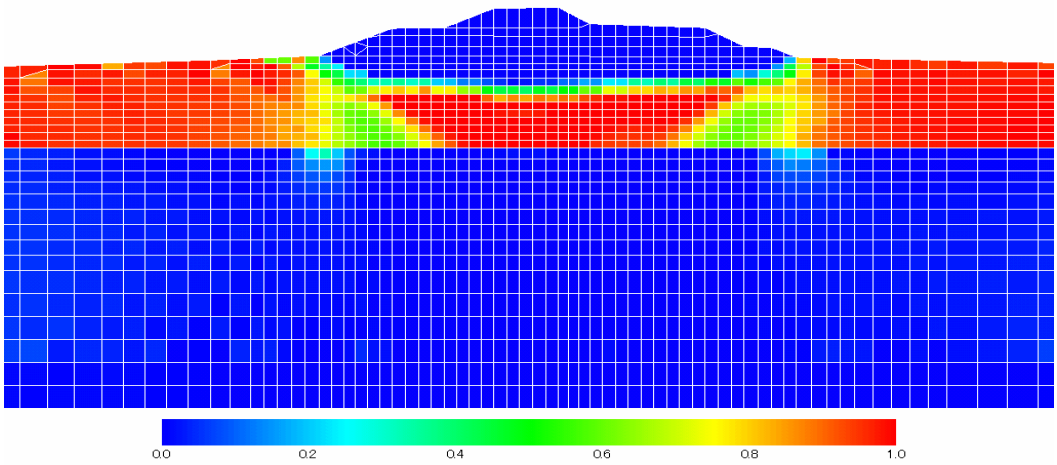

(b) Tonankai-Tokai Coupled Eq.

Figure 6. Distribution of excess pore water pressure ratios at the end of the earthquake.

The time histories of excess pore water pressure ratios of elements P1 (at the depth of 7 m in the free field) and P2 (at the same depth below the levee center) in 'As' are shown in Figure 7. It is obvious that the seismic loadings induce a typical pattern of liquefaction response of the soil layer with excess pore pressure ratios approaching 1.0 and remaining high thereafter.

A comparison between Sekigahara-Yoro earthquake and Tonankai-Tokai coupled earthquake shows that the magnitude of acceleration has a significant effect on the rate of the generation of excess pore water pressures. Due to much larger initial acceleration as depicted in Figure 2, the liquefiable sand under Sekigahara-Yoro earthquake produces a rapid response of excess pore water pressure buildup and leads to full liquefaction state earlier.

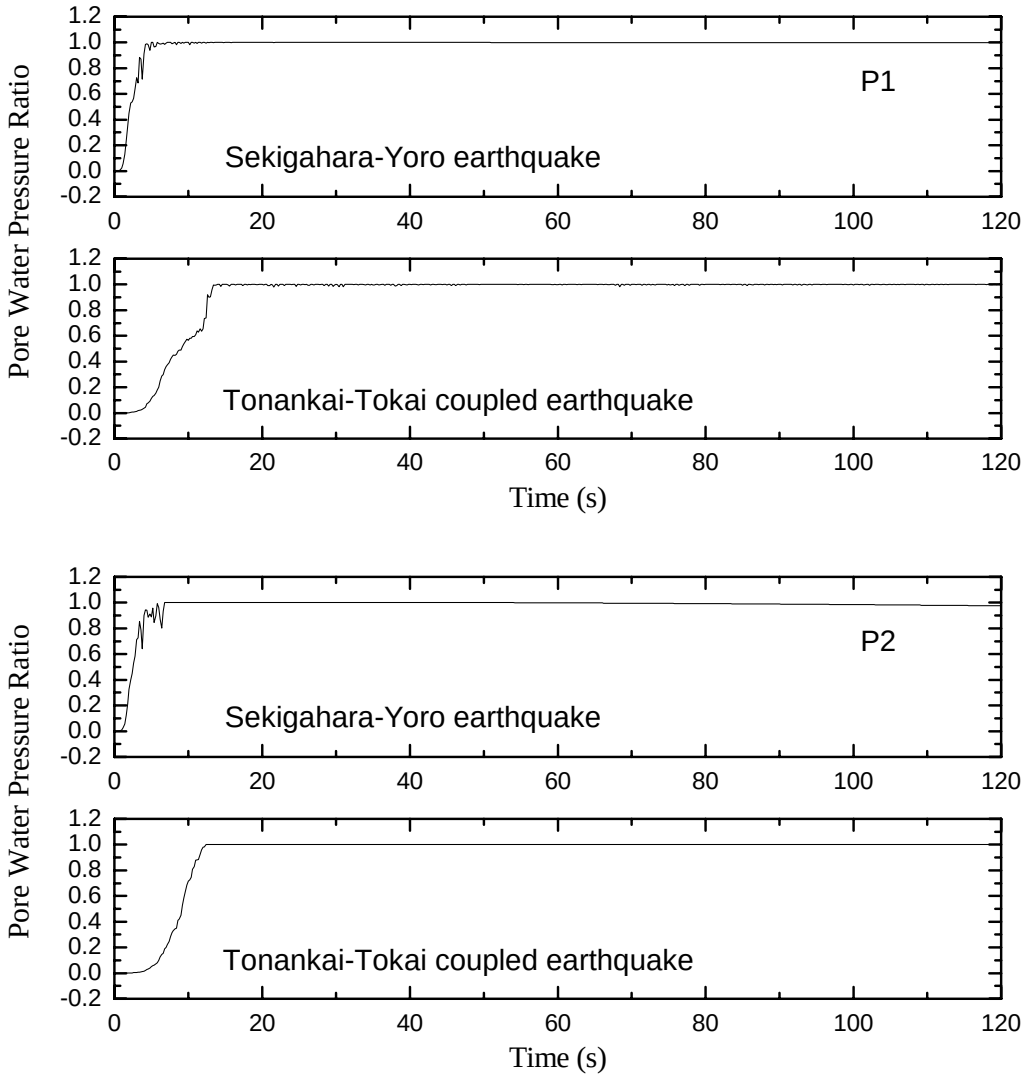

Figure 7. Time histories of excess pore water pressure ratios.

Accelerations

The accelerations at two representative locations (crest and toe), are depicted in Figure 8 respectively. It shows a rapid decrease which results from soil stiffness degradation due to excess pore water pressure generation. It is worth noting that the acceleration response of the toe and crest of the levee still maintains a low amplitude even after the free field attained full liquefaction. The result is in keeping with the dilative response of the foundation soil during the earthquake loadings.

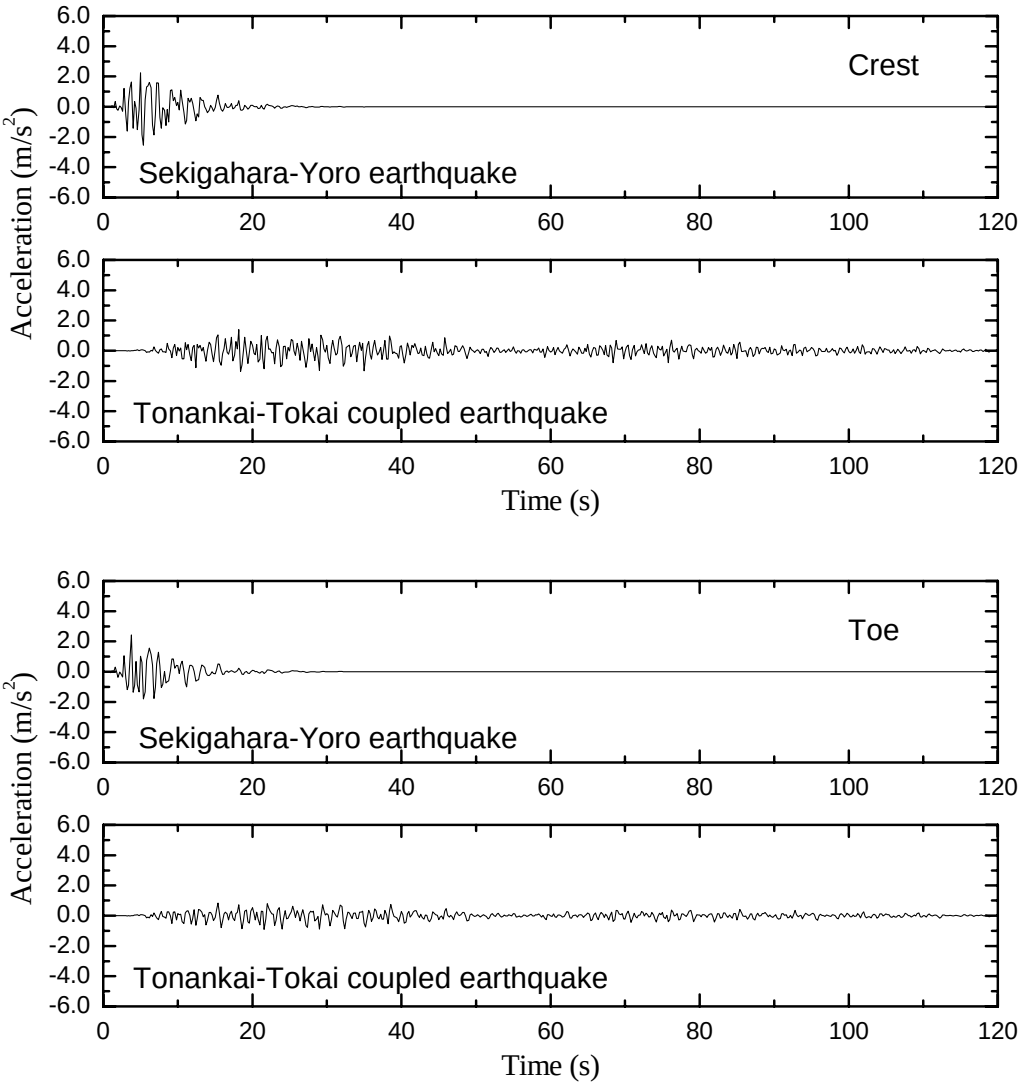

Figure 8. Acceleration time histories at two representative locations.

Deformations

Figure 9 shows the deformed configuration of the levee-foundation system at the end of the earthquake. The settlement histories of the levee toe and crest are illustrated in Figure 10. From the two deformation patterns under both earthquakes, some characteristics can be concluded that: (1) the extensive liquefaction causes a typical lateral spreading of the foundation soil towards the free field; (2) the crest undergoes large settlements due to the combined action of the migration of underlying foundation soil and the deformation of the levee itself; (3) due to initial static shear stresses induced by the levee weight, the foundation soil below the levee toe suffers severe deformations. Particularly, although Tonankai-Tokai coupled earthquake takes longer to trigger liquefaction than the active fault earthquake, the deformations occurring under Tonankai-Tokai coupled earthquake are significantly large compared with those under Sekigahara-Yoro earthquake. The reason is that the duration of excitation after the ground reach liquefaction is much longer for Tonankai-Tokai coupled earthquake than the active fault earthquake. Therefore, it is indicated that the duration of the excitation after the ground reach liquefaction is one of the most important factor for settlement.

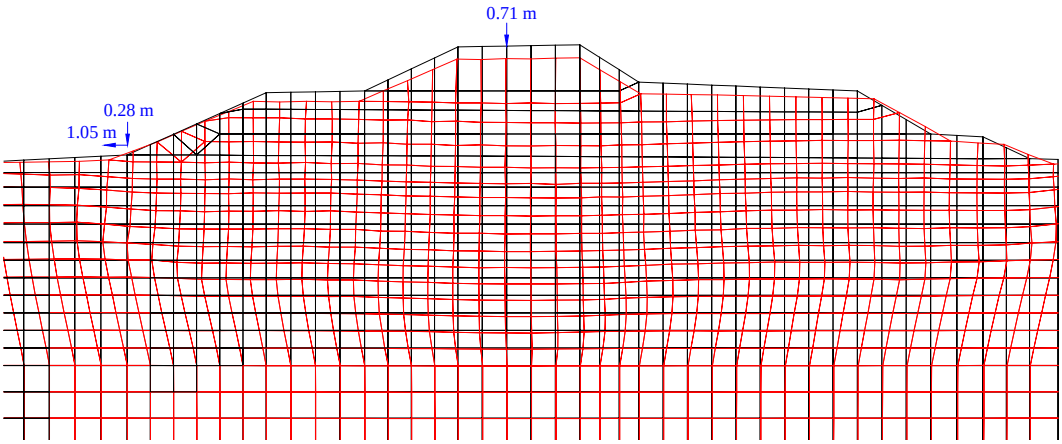

(a) Sekigahara-Yoro Eq.

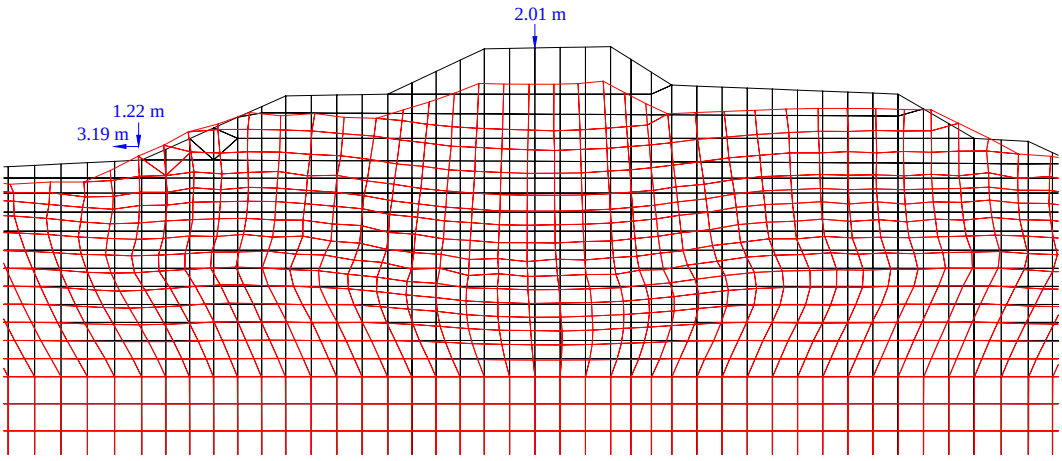

(b) Tonankai-Tokai Coupled Eq.

Figure 9. Configuration of the levee at the end of the earthquake.

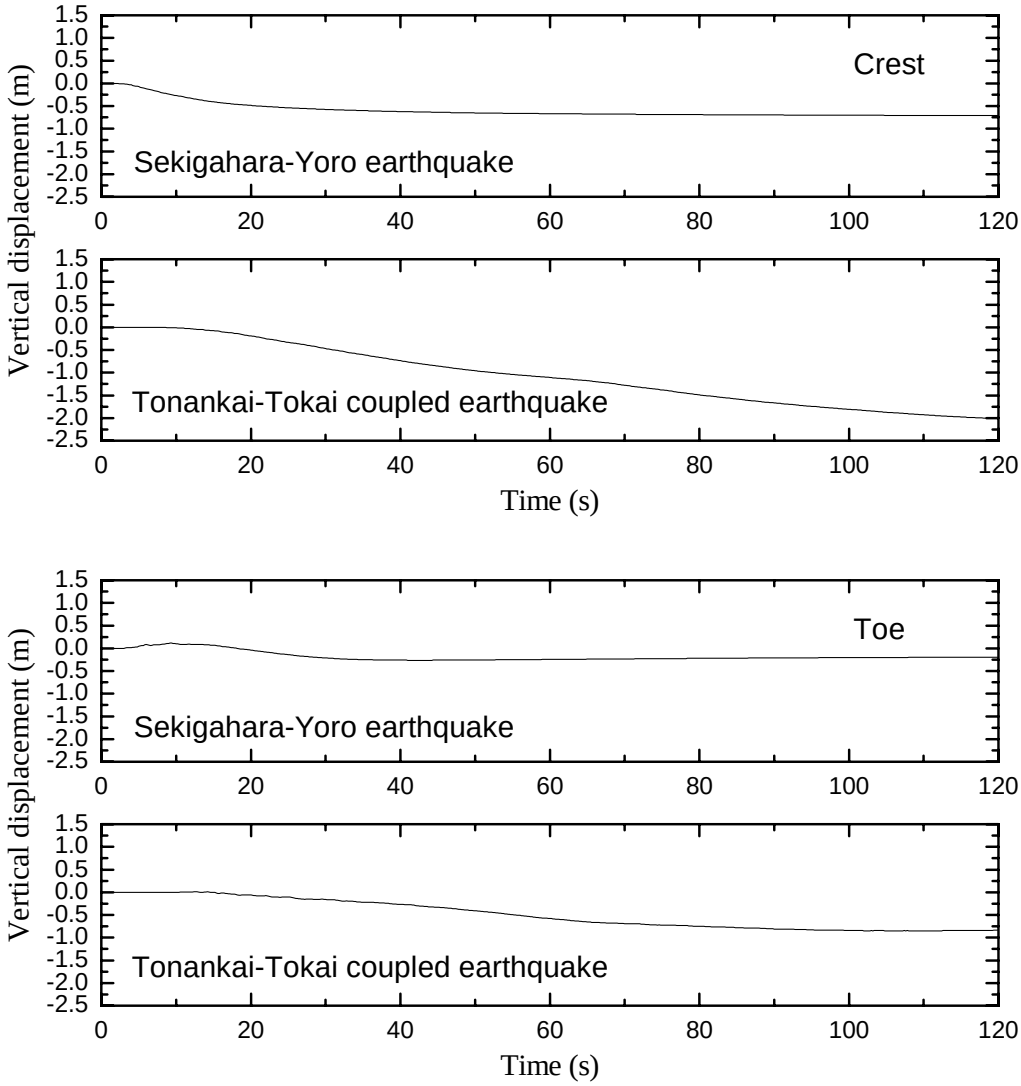

Figure 10. Time histories of settlements.

Figure 11 presents computed shear stress–strain with focus on the representative spatial elements in P1, in the free field and P2, below the levee center. The results reveal that the sand exhibits a significant degradation of shear stiffness and strength with cycle-by-cycle permanent shear strain accumulation because of liquefaction. Regarding the effect of duration of the excitation on the deformation of the soil, these simulation results show good agreement with the above views in Figure 10.

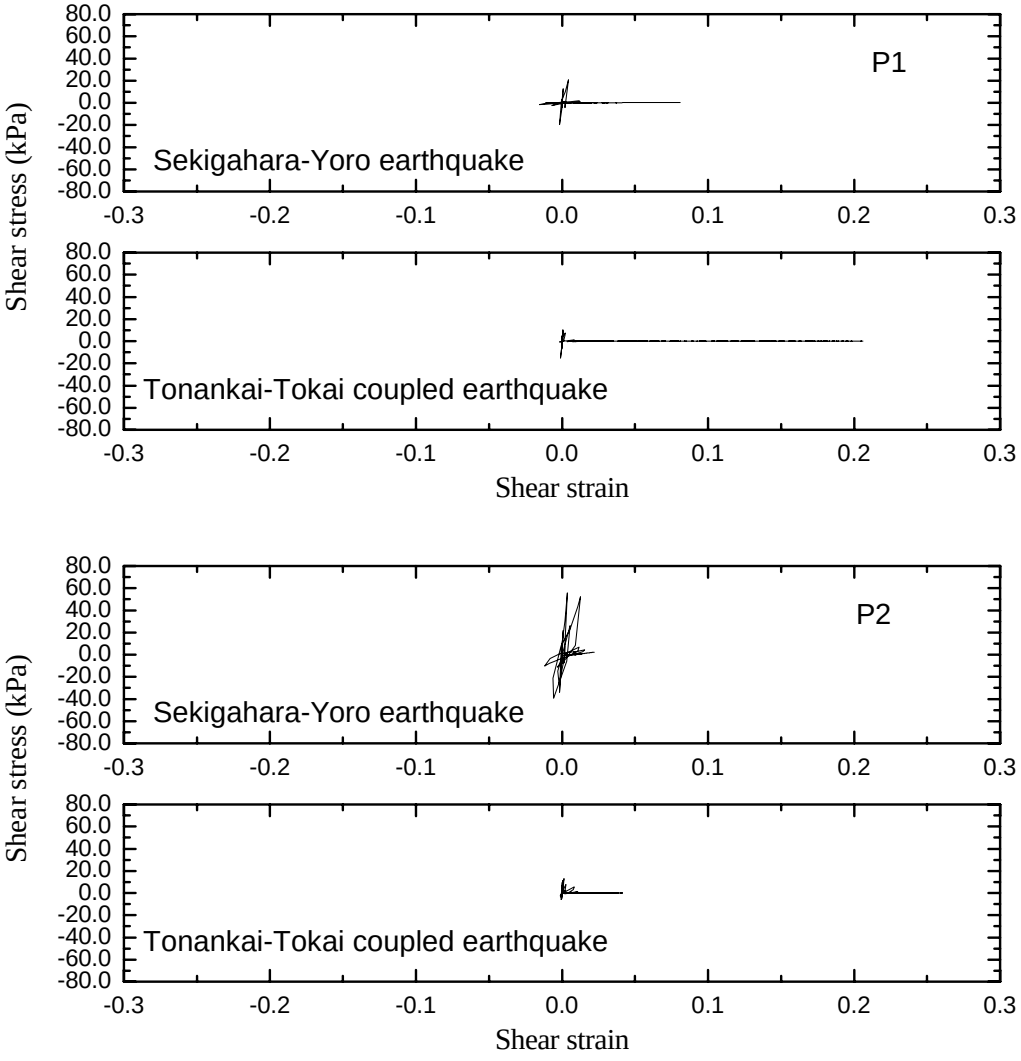

Figure 11. Histories of shear stress–strain.

CONCLUSIONS

In this study, effective stress based finite element analyses are carried out by program code "LIQCA" to compare the liquefaction-induced settlement of the river levees by both Tonankai-Tokai coupled earthquake and Sekigahara-Yoro Fault earthquake.

From the numerical results, it is found that the long-duration earthquake represented by Tonankai-Tokai coupled earthquake gives much large settlement of the river levee than the short-duration earthquake represented by the near-field active fault earthquake. Tonankai-Tokai coupled earthquake takes longer to trigger liquefaction than the active fault earthquake. The duration of excitation after the ground reach liquefaction is much longer for Tonankai-Tokai coupled earthquake than the active fault earthquake. It is concluded that the duration of the excitation after the ground reach liquefaction is one of the most important factor for settlement.

REFERENCES

Biot, M.A. "General theory of three-dimensional consolidation," Journal of Applied Physics, 12-4, 155-164, 1941.

Creager,P., Justin,D. and Hinds,J., Engineering for Dams, Vol.3, Earth, Rock-Fill, Steel and Timber Dams, pp.647-650, 1945.

Kameda,H. "Evolutionary spectra of seismogram by multi-filter, Journal of Engineering Mechanics Division, ASCE, **101**, 787-801, 1975.

The LIQCA Research and Development. "User's manual for LIQCA2D04," 2005.

National Disaster Prevention Council. "Report by Special Survey Committee on Tokai Earthquake," 2001. (in Japanese).

Oka, F., Yashima, A., Shibata, T., Kato, M. and Uzuoka, R. "FEM-FDM coupled liquefaction analysis of a porous soil using an elasto-plastic model," Applied Scientific Research, 52, 209-245, 1994.

Oka, F, Yashima, A., Tateishi, A., Taguchi, Y. and Yamashita, S. "A cyclic elasto-plastic constitutive model for sand considering a plastic-strain dependence of the shear modulus," Geotechnique, 49-5, 661-680, 1999.

Sugito, M., Furumoto, Y. and Sugiyama, T. "Strong Motion Prediction on Rock Surface by Superposed Evolutionary Spectra," Proc. of the 12th WCEE, CD-ROM, New Zealand, 2000.

The Headquarters for Earthquake Research Promotion. "Strong motion prediction for scenario earthquakes along the Nankai Trough," 2001. (in Japanese)

Zienkiewicz, O.C., Chan, A.H.C., Pastor, M., Schrefler, B. and Shiomi, T. "Computational Geomechanics", John Wiley & Sons, Chichester, 1999.